

DETERMINING INTRINSIC NOISE PARAMETERS OF 0.25 μm GATE PSEUDOMORPHIC HEMT

Indexing terms: Transistors, Semiconductor devices and materials, Noise, Modelling

An accurate equivalent circuit of a pseudomorphic HEMT (PM-HEMT) has been used, together with physically realistic values for the intrinsic PM-HEMT noise parameters (P , R , and C) to estimate the extrinsic noise parameters (minimum noise figure, optimum noise impedance, etc.) of a 0.25 μm gate PM-HEMT. It is demonstrated that good agreement with experiment can be obtained for the minimum noise figure, optimum noise impedance, and also noise resistance, over the frequency range 6–18 GHz.

Satellite communications systems operating at 12 GHz require low noise receivers, the vital component of which is a very low noise amplifier such as a submicrometre gate length MESFET or HEMT. Typically, noise figures of less than 0.9 dB are required, preferably with at least 10 dB of associated gain. These performance requirements are now being met by 0.25 μm gate length PM-HEMTs, which are replacing MESFETs because of their lower noise performance for the same gate length. To support the design of these devices, accurate noise models are required which can predict all the noise parameters of the PM-HEMT over a wide frequency range. In this Letter such an approach is demonstrated, and the feasibility of going from a physical noise model to accurate noise parameters is discussed.

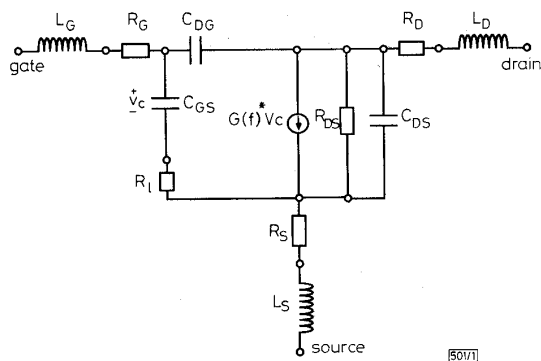


Fig. 1 Equivalent circuit representation of PM-HEMT

$G(f) = g_{m0} \exp(-j\omega\tau_d)$, where g_{m0} is DC transconductance, f is operating frequency, $\omega = 2\pi f$, and τ_d is time delay

Results are reported for the noise parameters of 0.25 μm gate length PM-HEMTs ($\text{Al}_x\text{Ga}_{1-x}\text{As}/\text{In}_y\text{Ga}_{1-y}\text{As}/\text{GaAs}$). The noise figure, optimum noise impedance and also noise resistance have been measured over the range 6–18 GHz using an automatic noise meter. In addition, S-parameter measurements, and the equivalent circuit fitting, of the same device have been carried out to give realistic values for the circuit elements shown in Fig. 1. All measurements were performed using 'on-wafer' probing to give the greatest accuracy. Using the equivalent circuit of Fig. 1, we have subsequently included current noise generators for gate and drain noise sources. The intrinsic noise of the PM-HEMT is specified in the usual way¹ via the parameters P , R , and C defined by

$$P = \frac{\langle i_d^2 \rangle}{4kT \Delta f g_m} \quad R = \frac{g_m \langle i_g^2 \rangle}{4kT \Delta f \omega^2 C_{gs}^2}$$

$$jC = \frac{\langle i_g^* i_d \rangle}{\sqrt{\langle i_d^2 \rangle \langle i_g^2 \rangle}} \quad (1)$$

where i_d and i_g are the drain and gate noise currents, g_m is the transconductance, C_{gs} is the source-gate capacitance, k is the Boltzmann constant, T is the temperature, Δf is the bandwidth, and $\omega = 2\pi f$, where f is the operating frequency.

By varying P , R , and C , and using the equivalent circuit estimated from S-parameter measurements, it is possible to

calculate the minimum noise figure and real and imaginary parts of the optimum impedance using the correlation matrix method,² and thus find the values of P , R and C that give the best fit to experiment. In fact, it is the optimum reflection coefficient Γ that is measured, and this is related to the optimum noise impedance Z_{opt} by

$$\Gamma = |\Gamma| e^{j\theta} = \frac{Z_{opt} - 50}{Z_{opt} + 50} \quad (2)$$

For the device discussed here, the required values of P , R , and C were found to be $P = 1.0$, $R = 0.4$, and $C = 0.79$ at 12 GHz.

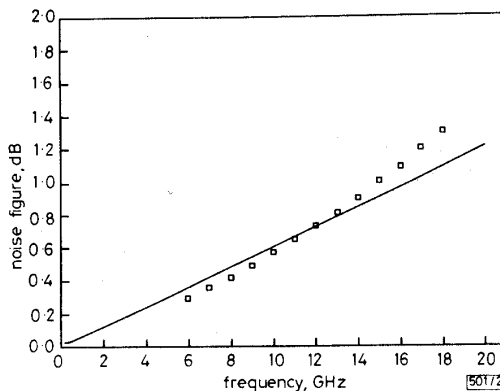


Fig. 2 Graph of noise figure against frequency

Equivalent circuit shown in Fig. 1

These values are well within the expected range predicted by physical noise models.^{3,4} Further, these values were also found to fit the noise figure, $|\Gamma|$ and θ over the whole measured frequency range 6–18 GHz (Figs. 2–4). In addition, although no attempt was made to adjust the values of the PM-HEMT noise parameters to fit the noise resistance, the

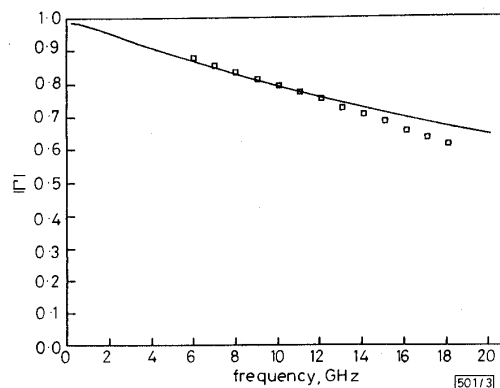


Fig. 3 Graph of modulus of optimum reflection coefficient against frequency

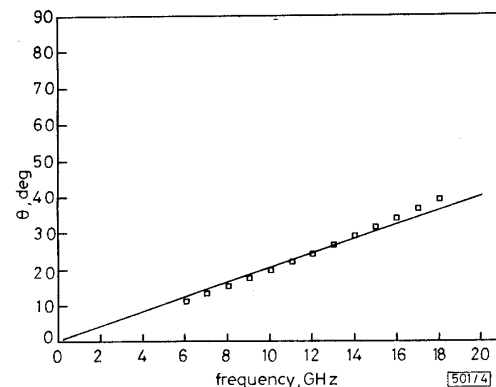


Fig. 4 Graph of θ (angle of optimum reflection coefficient, Γ , where $\Gamma = |\Gamma| e^{j\theta}$) against frequency

values for P , R and C quoted above gave excellent agreement with experiment for the noise resistance, again over the frequency range 6–18 GHz (Fig. 5).

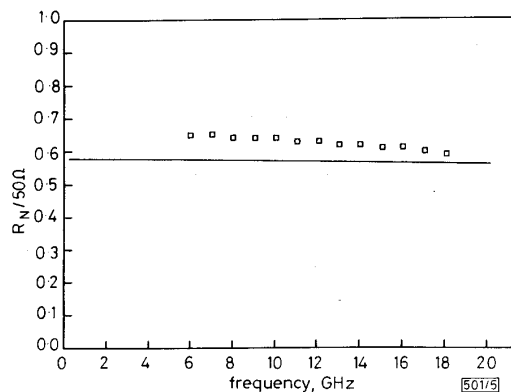


Fig. 5 Graph of noise resistance (normalised to 50 Ω) against frequency

We believe this is the first report that demonstrates that the inclusion of physically realistic intrinsic PM-HEMT noise parameters into an accurate PM-HEMT equivalent circuit predicts not only the noise figure, but also the optimum noise impedance and noise resistance, giving excellent agreement with experiment over a wide frequency range, when fitted at only one frequency.

Previous efforts to compare noise models with experiments have generally concentrated on just calculating the minimum noise figure at spot frequencies,⁵ using equivalent circuits which are too simple to be able to simulate a realistic PM-HEMT. For example, in the original paper by Pucel,¹ the gate-drain capacitance and output conductance and capacitance were not taken into account.

The results of this work suggest that it should be possible to go directly from a physical noise model (which requires input layer thicknesses, doping densities, mobilities, saturation velocities etc.) to accurate predictions of noise figure, optimum noise impedance, and noise resistance, provided that a reasonably accurate equivalent circuit model of the PM-HEMT is known. The reason for not using such an approach here is that the numerous parameters entering the physical model, and their uncertainties, are such that, at present, it is not possible to calculate P , R , and especially C , to the accuracy required to fit to experiment. Nevertheless, the results of this work suggest that such an approach is feasible in principle. (The reason why the correlation coefficient C needs to be known to high accuracy is that it appears in the noise expressions as the factor $(1 - C^2)$, and because C is likely to be in the range 0.7–0.95, small differences in C can result in large differences in the predicted noise figure, optimum impedance, etc.).

In conclusion, we have demonstrated the feasibility of going from a physical noise model, via a realistic equivalent circuit (including gate-drain capacitance), to predicted values of noise figure, optimum noise impedance, and also noise resistance. In addition, we have shown that this approach is capable of giving an excellent fit to experimental measurements of the four noise parameters over a wide frequency range. It is also possible to investigate, using the same intrinsic noise parameters, the effect of the parasitics on the noise performance, and so use the noise model in a CAD role to predict the optimum PM-HEMT layout for low noise performance.

Acknowledgments: The authors would like to acknowledge partial support of this work by the EC ESPRIT II Basic Research Action 3017 ('NOISE') Project. The 0.25 μm PM-HEMT was fabricated and measurements performed by the staff of the GaAs division of GEC-Marconi Materials Technology.

R. I. TAYLOR
D. M. BROOKBANKS
A. J. HOLDEN

6th August 1991

GEC-Marconi Materials Technology Limited
Caswell, Towcester, Northants NN12 8EQ, United Kingdom

References

- 1 PUCCEL, R. A., HAUS, H. A., and STATZ, H.: 'Signal and noise properties of gallium arsenide field effect transistors', *Adv. Electron. Electron Phys.*, 1974, **38**, pp. 195–265
- 2 HILLBRAND, H., and RUSSEK, P. H.: 'An efficient method for computer aided noise analysis of linear amplifier networks', *IEEE Trans.*, 1976, **CAS-23**, pp. 235–238
- 3 CAPPY, A.: 'Noise modelling and measurement techniques', *IEEE Trans.*, 1988, **36**, pp. 1–9
- 4 ANDO, Y., and ITOH, T.: 'DC, small-signal, and noise modelling for two-dimensional electron gas field-effect transistors based on accurate charge-control characteristics', *IEEE Trans.*, 1990, **ED-37**, pp. 67–77
- 5 CAPPY, A., and HEINRICH, W.: 'High frequency FET noise performance: A new approach', *IEEE Trans.*, 1989, **ED-36**, pp. 403–409

IMPROVED BLOCK TRUNCATION CODING USING HOPFIELD NEURAL NETWORK

Indexing terms: Image processing, Neural networks

Block truncation coding (BTC), a recent technique used in the coding of image data, is based on the classification of pixels within a small image block into two classes. Earlier methods used statistical information for this classification. In the Letter, a new technique is introduced which uses a Hopfield neural network to define the pixel classes. Results are presented for four monochrome still images. The new algorithm is shown to provide improved performance when compared to the two previous BTC algorithms.

Introduction: Block truncation coding (BTC) for image compression was described by Delp and Mitchell in 1979.¹ Their method employed a 1 bit adaptive moment-preserving quantiser operating on small blocks (tiles) of the image. Using this original algorithm, the first-order and second-order moments of the original blocks were preserved. In 1985, Udpiker and Raina proposed a modified BTC algorithm for monochrome still images.² Their algorithm preserved only the first-order moments, and was shown to be optimum in the mean-square sense, among the class of BTC algorithms that use the 'local mean' as the threshold for the 1 bit quantiser.

We present a BTC algorithm with improved performance, achieved using a Hopfield neural network^{3–5} as the 1 bit quantiser. Performance improvement is demonstrated by presenting mean-square error (MSE) and signal-to-noise ratio (SNR) values for our algorithm and for the two algorithms referred to above,^{1,2} for four monochrome test images.

BTC algorithm:¹ The 1 bit quantiser threshold is given by

$$X_{th} = \bar{X} \quad (1)$$

and the quantiser output levels are

$$A = \bar{X} - \sigma \sqrt{\left(\frac{q}{n-q}\right)} \quad x(i) < X_{th}$$

$$B = \bar{X} + \sigma \sqrt{\left(\frac{n-q}{q}\right)} \quad x(i) \geq X_{th} \quad (2)$$

where $x(i)$ is the i th pixel value in the block, n is the number of pixels in the block, q is the number of pixels greater than or equal to X_{th} , \bar{X} is the block mean value, and σ is the standard deviation of the image block.

Modified BTC algorithm:² This method preserves only the first-order statistical information, namely the lower mean \bar{X}_L (the mean of the pixel values below the threshold) and the higher mean \bar{X}_H (the mean of the pixel values greater than or equal to the threshold). As in the original algorithm, the threshold is taken as the mean of the block pixel values.